On the Non-Destructive Testing of Metal Foams

H.P. Degischer, A. Kottar,
Institute of Materials Science & Testing, Vienna University of Technology, Vienna/Austria

Abstract

Closed cell aluminium and iron based foams produced by remelting foamable precursor material are chosen for experimenting non destructive test (NDT) methods. Open pores and cracks in the surface skin of foam samples are determined by dye penetrant tests. Eddy current and conventional ultrasonic testing were not successful in characterising the surface skin in more detail. X-ray transmission yields information on the heterogeneity of mass distribution, if two dimensional local mean mass density maps are computed. X-ray computed tomography (CT) provide data of the three-dimensional mass distribution. Three-dimensional local mean density maps are proposed to identify hard and soft regions in a cellular structure. High resolution CT enables a detailed structural analysis of the foam.

1. Introduction

Industrial production of foamed metals is now established for specific applications like stiff sandwich structures [1][2][3] or panels [4][5][6], casting inserts and crash absorbers [7][8], heat exchangers with open porosity [9]. Being in a developmental stage there are no generally acknowledged specifications and quality definitions have yet to be defined.

The criteria for specifications of metallic foams must be based on the property requirements [10], which can be correlated to structural features and their quantitative description. Some non-destructive test-methods (NDT) were applied to metallic foams with the aim to propose quality control methods for the development and manufacturing of reliable products.

2. Material

Samples of foamed aluminium and iron alloys with closed cell structure were chosen for testing. The ALULIGHT material [11][12][8] of AlSiMg (AA 6xxx) wrought and of AlSi12Mg cast alloys were produced by LK-Ranshofen [4] and by SAS-Bratislava [10] and are covered by a skin of the matrix alloy, respectively its oxide. The iron based samples had been foamed with $SrCO_3$ in an open container at TU-Vienna [13].

3. NDT-Methods

3.1. Dye Penetrant Test and Eddy Current Test

Dye penetrant relies on surface defects being capable of absorbing liquid, retaining this and highlighting the defect by applying a colouring developer [14]. Commonly used penetrant and developer were applied to original surface skins of differently foamed ALULIGHT samples. The appearance of the coloured marks was recorded in function of time and their number densities were determined well before full development. Eddy-current tests on non-magnetic

J. Banhart, M.F. Ashby, N.A. Fleck: *Metal Foams and Porous Metal Structures.* © MIT Verlag (1999)

materials yield signals according to changes in conductivity, surface roughness and geometrical features [14]. ALULIGHT skins were tested by small probe coils applying up to 25 kHz and observing the impedance by an oscilloscope.

3.2. X-Ray Radiography

In transmission radiography the recorded intensities provide an integral information about the attenuation of the X-ray beam along its path, whereas in CT the recording of intensities from a large number of different views allows the mathematical reconstruction of the local attenuation at any point of the object [15]. For both methods the attenuation values can be correlated to the mass density if the material composition is known. The following X-ray sytems have been used: a Philips Tomoscan SR7000 medical tomograph to provide digital transmission radiography and computed tomography as well; a technical SMS-Tomograph [16] and a GAMMASCAN micro-CT system [17].

Two dimensional (2D) local mean mass density maps of flat parts were derived from transmission images by averaging over a surrounding area of $n \times m$ pixels. CT experiments reveal a three dimensional (3D) data set of volume elements (voxels) containing the 3D mass distribution of the tested object. This data set is appropriate to investigate the cellular structure [18][19] and to calculate a mean local density function [20] by averaging over a certain surrounding volume of each voxel.

4. Results

4.1. Surface Quality Tests

The open pores detected by the dye penetrant test method in the skin of ALULIGHT samples (Fig. 1) measure from 0,1 mm to about 2 mm in diameter. Fig. 2 compares the number density of open surface pores of the freely foamed sample (Fig. 1a) and the sample foamed vertically in a mould (Fig. 1b) where the pore density increases in the direction of material flow. Samples, which were foamed horizontally in a mould starting from rod like precursor material, exhibit essentially pore free regions, where the oxide skins of the precursor material form the foams' surface. In-between, pores appear in densities of several open pores/cm^2. The distribution of the open pores in the surface skin depends on the foaming conditions. Surface cracks can also be visualised by the dye penetrant method.

The impedance signals of Eddy-current tests varied significantly while scanning an ALULIGHT surface, but the only well defined effect was that associated with surface cracks. The superposition of the electromagnetic effects of surface roughness, local variations of the oxide skin and of the cellular structure underneath could not be unfolded for evaluation.

4.2 Local Mass Distributions

Fig. 3a demonstrates a digital recording of the X-ray intensity transmitted through a part of a cellular wrought alloy slab ($200 \times 130 \times 20$ mm^3, average density ρ_m = 0.57 g/cm^3) with skin (same sample as Fig. 1b). The intensity in each pixel oscillates strongly, which complicates the interpretation of local density variations. The contour plot of 2D local mean density is shown in Fig. 3b varying from less than 0,2 g/cm^3 to more than 2 g/cm^3. It was computed by averaging the mass densities over columns of the cross section of 11×11 pixels ($6{,}4 \times 6{,}4$ mm^2) and the height of the sample's thickness. The example reveals the drainage effect the sample suffered by foaming in an upright position. Some big cells (>4mm) are visible too.

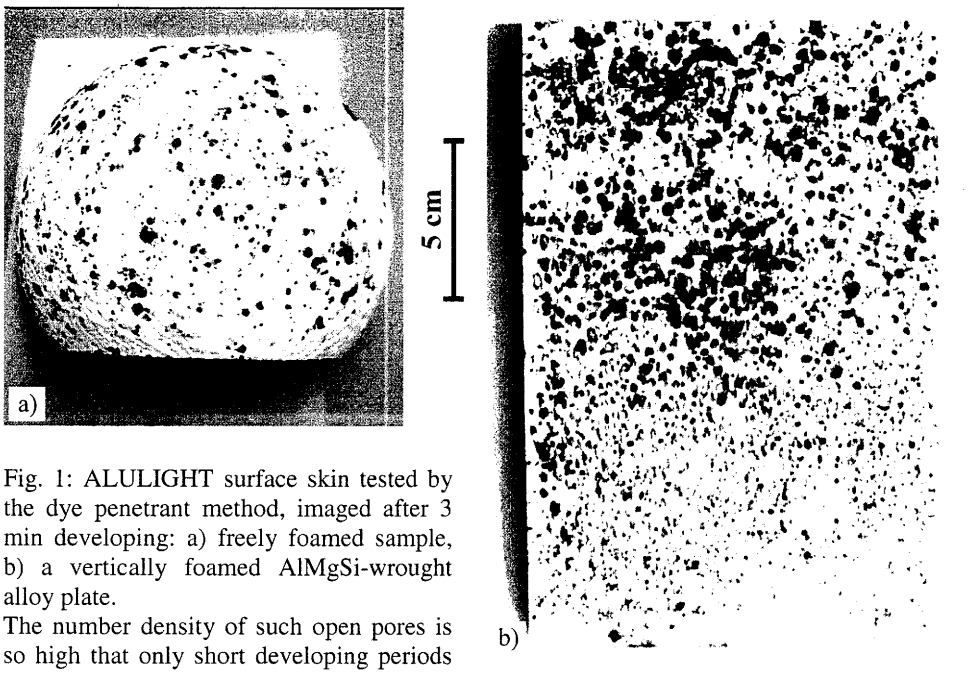

Fig. 1: ALULIGHT surface skin tested by the dye penetrant method, imaged after 3 min developing: a) freely foamed sample, b) a vertically foamed AlMgSi-wrought alloy plate.
The number density of such open pores is so high that only short developing periods (< 3 min) allow the counting of the individual marks before merging with each other starts.

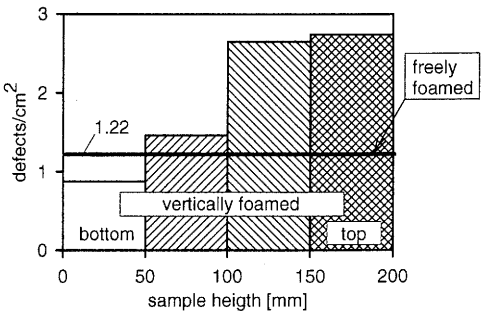

Fig. 2: Number density of dye penetrant spots comparing the freely foamed sample with the vertically foamed plate (Fig. 1); in the latter the surface is divided in areas of 50 mm in height.

X-ray transmission pictures of ALULIGHT samples on a screen did not clearly reveal intentionally drilled holes of a diameter of a quarter of the sample's thickness. The radiography of the transmitted intensity perpendicular to the holes in Fig. 4a indicates the density variation caused by the drilled holes faintly. Fig. 4b shows a cross section of that sample in beam direction recorded by X-ray computed tomography, which shows clearly the holes and the inhomogeneous distribution of the material, especially close to the surface.

Medical CT can be applied to cellular aluminium yielding a resolution of about 0,7mm (See comparison with a metallographic light microscopic picture in Fig. 5). The main features of the cellular structure can be revealed even in X-rayed cross sections of more than 250 mm in diameter. Fig. 6 shows a cross section of an iron based foam.

3D-CT recordings of cellular metals serve as basis for 3D density mappings. Fig. 7 depicts the mass distribution recorded by CT along 3 perpendicular cross sections of the same sample as shown in Fig. 3. Fig. 7a represents the mass distribution in each voxel. Fig. 7b shows the corresponding 3D mean local mass density maps for the voxels along these cross sections. The cells bigger than 4 mm can be clearly identified even in the 3D mean local density map.

Mass density limits can be defined in 3D mean local density maps to distinguish regions with high or low mass density. Mean local density values of volumes of $2 \times 2 \times 2$ mm^3 of an

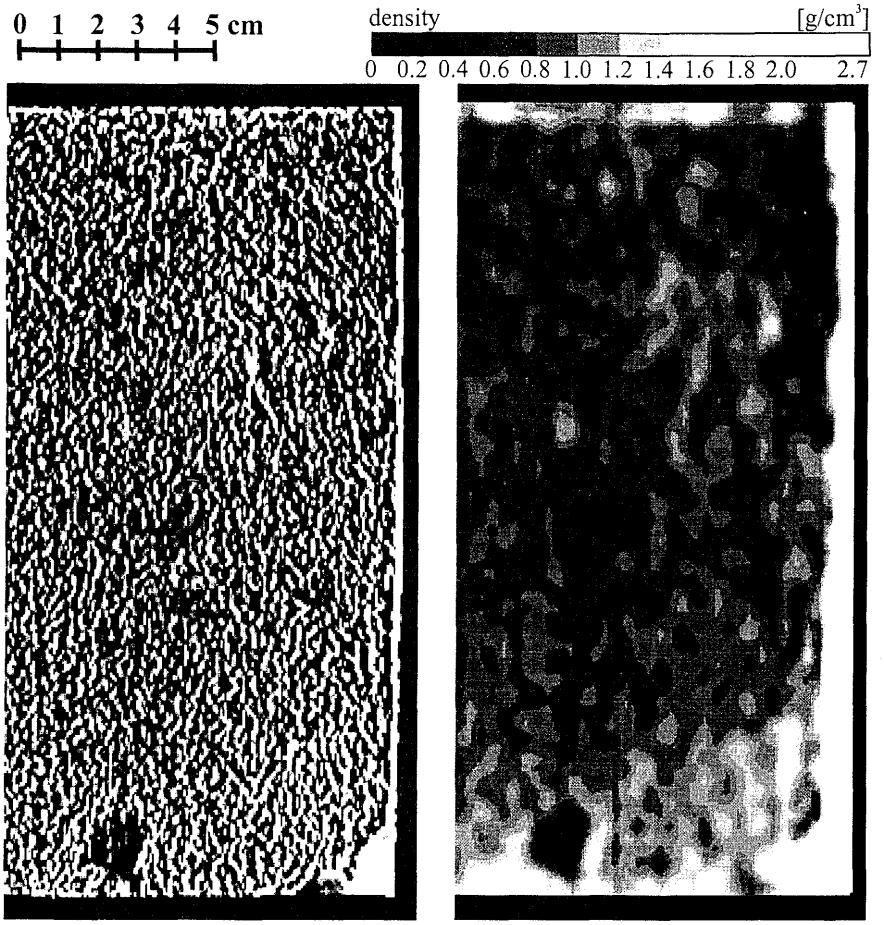

Fig. 3: X-ray transmission of ALULIGHT plate: a) transmitted intensity of each pixel (0,6 × 0,6 mm²); b) contour plot of the 2D mean local mass density.

AlSi12-ALULIGHT compression test sample measuring $22 \times 22 \times 30\,mm^3$ had been computed. A lower limit of 1,67-times the average density of the sample ρ_m was chosen to discriminate "hard" regions of higher mass density. The iso-surface in Fig. 8a encloses the voxels with values above that limit. The density limit is reduced to $1{,}33 \cdot \rho_m$ and the averaging volume is increased 27-times yielding the iso-surface given in Fig. 8b. Fig. 8a and b demonstrate the influence of the chosen density limit in combination with the averaging volume of the mean local density mapping. The influence of the selection of the averaging volume alone on the localisation of "soft" regions is compared in Fig. 8c and d, where the iso-surface at $0{,}67 \cdot \rho_m$ encloses the regions of lower mean local mass density. The averaging volume is changed from a cube of $6 \times 6 \times 6\,mm^3$ in Fig. 8c to a more than twice as big parallelepiped with one third of the edge lengths of the sample, i.e. $7 \times 7 \times 10\,mm^3$ in Fig. 8d. The smaller the averaging volume the bigger the scatter in mean local density will be.

The iso-surface presentations of the limits of mean local mass density reveal as well the 3D arrangement of the corresponding hard or soft regions across the sample. Fig. 8b shows a V-like interconnection of hard regions across the sample, which will increase the compression

resistance in the long direction. The soft regions of that sample - see Fig. 8c, d - are oriented rather parallel to the direction of compression suggesting, that they will not be identical with deformation bands [21]. Consequently the spatial distribution of hard and soft regions has to be considered too as an additional quality criterion.

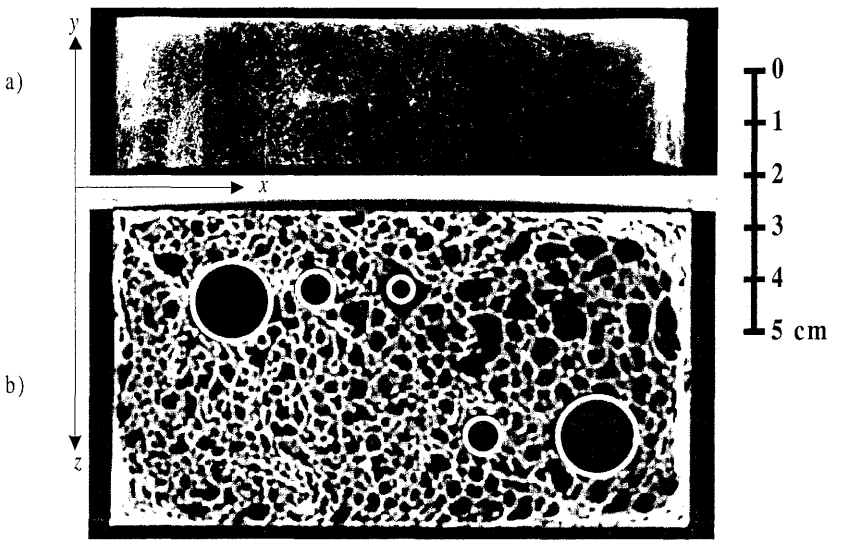

Fig. 4: ALULIGHT sample with drilled holes (explanation see text).

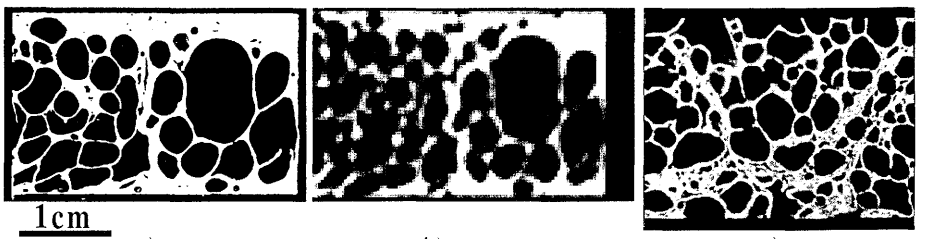

Fig. 5: Comparison of cross sections of ALULIGHT recorded by: a) light microscopy of a cellular wrought alloy, b) medical CT of the same area, c) high resolution CT (voxelsize $40\times40\times40\,\mu m^3$) of a cellular casting alloy.

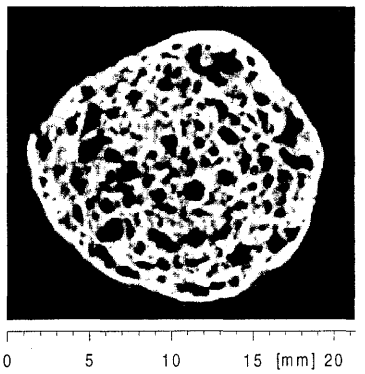

Fig. 6: Fan beam CT contrast of a cellular iron based sample of about 15 mm diameter [13] obtained by 450 kV X-ray tube [16] yielding a resolution of 0,1mm.

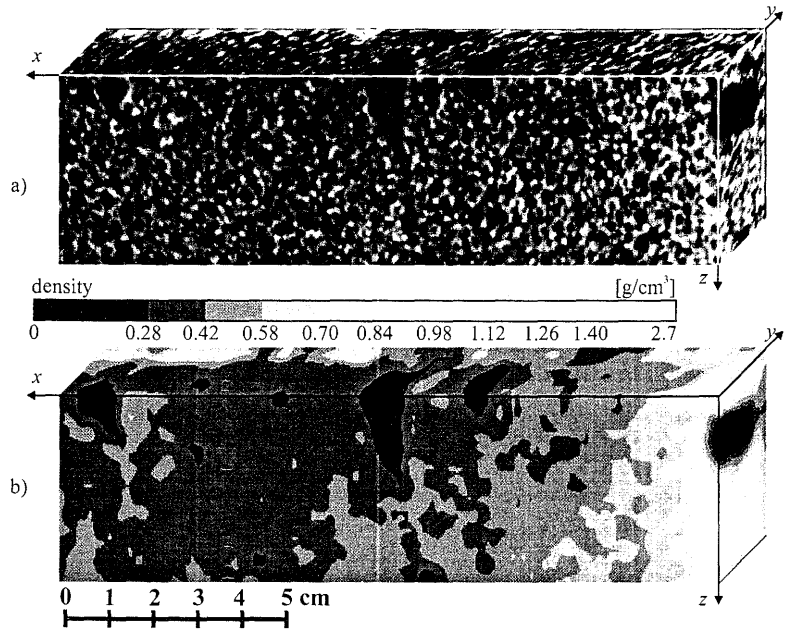

Fig. 7: Mass density distribution on the surfaces of a parallelepiped recorded by technical CT: a) CT cross section images from the 3D data set (voxelsize 0,3×0,3×0,3 mm³), b) contour plots of 3D mean local density maps for an averaging volume of 4,3×4,3×4,3 mm³ (15×15×15 voxels) for the voxels along the planes shown in (a).

High resolution CT reveals details in the cellular structure as shown in Fig. 5c: Cell walls down to about 100 µm thickness can be imaged in cross sections as well as tiny shrinkage pores in cell wall nodes. Such CT data can be used to study deformation mechanisms by computing 3D-displacements of structural features [22]. The 3D cellular structure can be represented by iso-surfaces illustrating the surface of cell boundaries (Fig. 9).

5. Discussion of the Investigated NDT Methods

The dye penetrant method reveals all open pores and cracks in the surface skin of ALULIGHT type material. From this the foaming flow during fabrication can be deduced. Eddy current tests reveal cracks in the surface skin and may have a potential of revealing more details on the consistence of the surface skin. Conventional ultrasonic testing could not be exploited to provide information on the cellular structure.

X-ray transmission images of cellular samples are ambiguous in detecting big pores. Any conventional X-ray transmission system including medical CT is suitable for identification of density variations of cellular metallic parts of regular shape, based on 2D mean local density maps. 3D X-ray computed tomograms of moderate resolution provide the basis for the calculation of 3D mean local mass densities to identify soft and hard regions and their spatial arrangement within the component. Density variation limits can be chosen as quality criteria, but have to be combined with a reasonable choice of averaging volume. The assessment of the spatial arrangement of such hard and soft regions in mechanically loaded components requires meso-mechanical simulation [21] and experience from mechanical testing [9][23]. High

resolution technical CT is a powerful research tool to characterise structural features in 3D to correlate them to materials properties and their scatter [9][22] and to stimulate modelling [24].

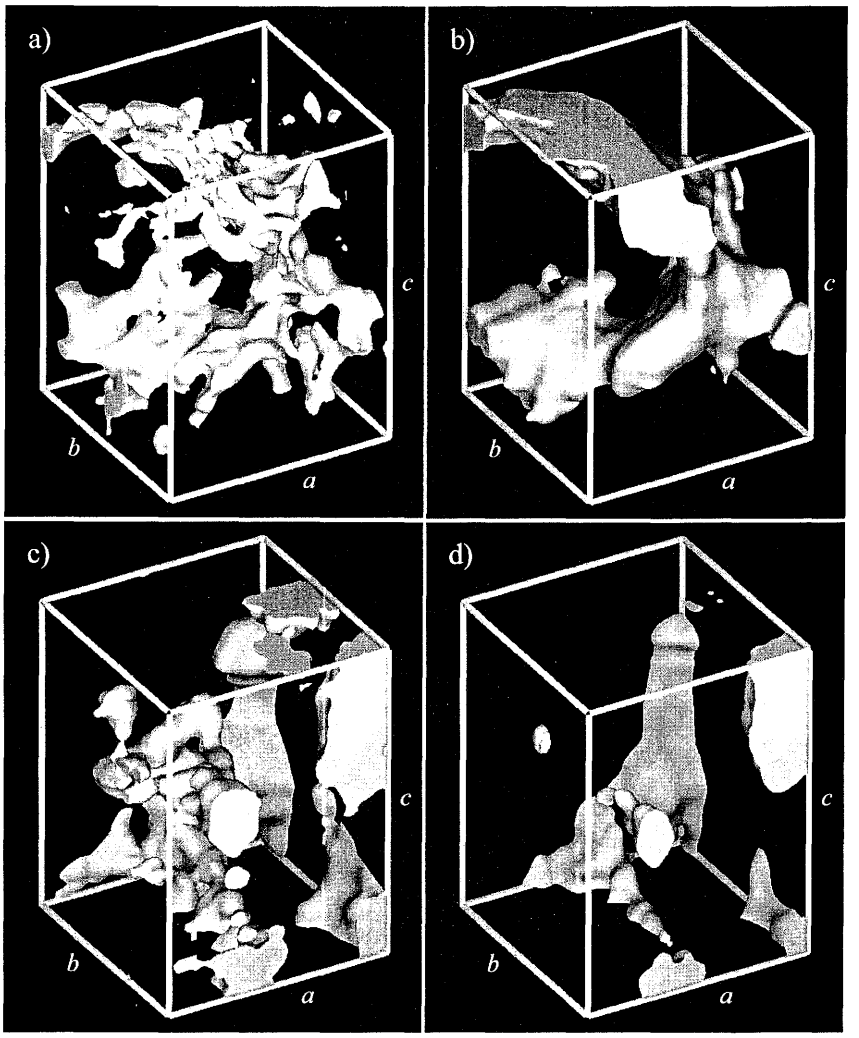

Fig. 8: Iso-surfaces of mean local mass densities in a AlSi12-ALULIGHT test sample ($a = b =$ 22 mm, $c = 30$ mm) of average density $\rho_m = 0.5$ g/cm^3: a) hard regions of mean local densities $\rho > 1{,}67 \cdot \rho_m$ in averageing volumes of $2 \times 2 \times 2$ mm^3, b) hard region of $\rho > 1{,}33 \cdot \rho_m$ within $6 \times 6 \times 6$ mm^3, c) soft regions of $\rho < 0{,}67 \cdot \rho_m$ within $6 \times 6 \times 6$ mm^3 d) same density limit as (c) but within $7 \times 7 \times 10$ mm^3 , i.e. 1/3 of the edge lengths of the sample.

Acknowledgements

The authors gratefully acknowledge: the provision of ALULIGHT samples by Leichtmetall-Kompetenzzentrum Ranshofen (A) and Slovak Academy of Science, Bratislava (SK); the execution of surface tests by the Institute for Testing and Research in Materials Technology, Vienna University of Technology (A); the admission to use CT at the Department of

Radiology, Division of Osteoradiology, University of Vienna (A), the Ferderal Institute for Materials Research and Testing , Berlin (D) and the Swiss Federal Laboratories for Materials Testing and Research, Dübendorf (CH). The work was funded by the Austrian Ministry of Science and Transport.

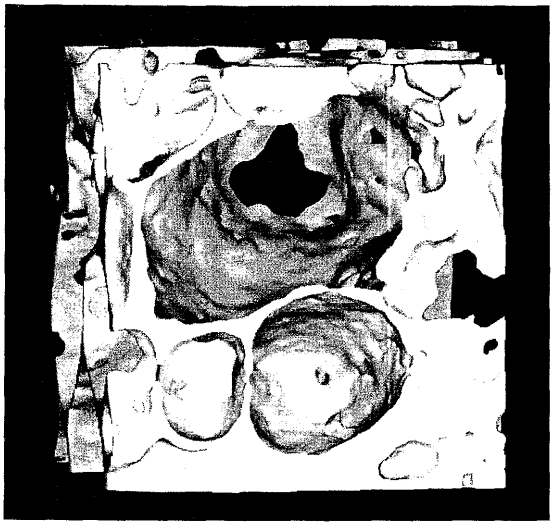

Fig. 9: Iso-surface at a level of 50% of ρ_{Al} computed from high resolution 3D technical CT data (voxelsize: $40\times40\times40\,\mu m^3$).

The volume of $8\times8\times8\,mm^3$ within a casting alloy ALULIGHT sample (same as in Fig. 8) shows a few cells, where the roughness of the cell walls, defects in cell walls, shrinkage pores in nodes and an ensemble of neighbouring cells can be seen.

References

[1] F. Baumgärtner, H. Gers, this conference
[2] W. Seeliger, this conference
[3] D.S. Shih, D.S.Schwartz, R.J.Lederich, L.Busche, D.A.Deuser, B. Norris, this confer.
[4] R. Kretz, E. Hombergsmeier, K. Eipper, this conference
[5] "Alulight", 1996, Mepura Leaflet, Ranshofen/Austria
[6] T. Miyoshi, M. Itoh, S. Akiyama, A. Kitahara, this conference
[7] P. Asholt, this conference
[8] T. Höpler, F. Schörghuber, F. Simancik, this conference
[9] A.G. Evans, this conference
[10] F. Simancik, this conference
[11] J. Banhart, J. Baumeister, M. Weber; Aluminium 70 (1994), 209-212.
[12] H.P. Degischer, F. Simancik; in "Environmental Aspects in Mat.Science", ed. H. Warlimont, DGM-Oberursel (1994), 137-140.
[13] B. Kriszt, A. Falahati, H.P. Degischer; in „Int. Konf. ST-W-WP-BM-QM", Hrg. S. Felber, T. Varga, J.L Zeman, TU-Vienna (1997) Bd. 2, 701-722.
[14] S. Steeb, Zerstörungsfreie Werkstück- u. Werkstoffprüfg., 1993, 2. Ed., Expert Verlag
[15] D. Copley, J.W. Eberhard, A. Mohr , 1994, Journal of Materials, **46** (1), 14-26.
[16] Industrial X-ray Computed Tomography, EMPA Leaflet, 1992
[17] Computertomographie, BAM Leaflet, 1997
[18] F. Grote, A. Schievenbusch, M. Mathes, this conference
[19] E. Cornelis, A. Kottar, A. Sasov, D. Van Dyck, this conference
[20] B. Kriszt, A. Kottar, H.P. Degischer, 1998, Werkstoffwoche '98, Vol. 8, 687-692.
[21] B. Kriszt, B. Foroughi, K. Faure and H.P. Degischer, this conference.
[22] B. Foroughi, 1998, Junior Euromat.
[23] B. Zettl, S. Stanzl-Tschegg, this conference.
[24] T. Daxner, H.J. Boehm, F.G. Rammerstorfer, this conference